Thermodynamics of isotropic and anisotropic layered magnets: Renormalization-group approach and 1/*N* expansion

V. Yu. Irkhin and A. A. Katanin*
Institute of Metal Physics, Ekaterinburg 620219, Russia
(Received 28 April 1997)

The $O(N)$ model of layered antiferromagnets and ferromagnets with a weak interlayer coupling and/or easy-axis anisotropy is considered. A renormalization-group (RG) analysis in this model is performed, the results for $N=3$ being expected to agree with those of the $1/M$ expansion in the CP^{M-1} model at $M=2$. The quantum and classical cases are considered. A crossover from an isotropic two-dimensional (2D)-like to a three-dimensional Heisenberg (or 2D Ising) regime is investigated within the $1/N$ expansion. Analytical results for the temperature dependence of the (sublattice) magnetization are obtained in different regimes. The RG results for the ordering temperature are derived. In the quantum case they coincide with the corresponding results of the $1/N$ expansion. The numerical calculations, based on the equations obtained, yield a good agreement with experimental data on the layered perovskites La_2CuO_4, K_2NiF_4, and Rb_2NiF_4, and the Monte Carlo results for the anisotropic classical systems. [S0163-1829(97)03946-5]

I. INTRODUCTION

The problem of layered magnetic systems is of interest both from theoretical and practical point of view. Here belong, e.g., quasi-two-dimensional (quasi-2D) perovskites,[1] ferromagnetic monolayers and ultrathin films.[2] Such systems possess magnetic transition temperatures that are low in comparison with the intralayer exchange parameter J and are determined by magnetic anisotropy and/or interlayer coupling.

The crucial role in the thermodynamic behavior of systems with small interlayer coupling (or anisotropy) belongs to the temperature crossover from a ''2D-like'' (isotropic) regime to the critical 3D (or 2D Ising) regime, respectively (see, e.g., Refs. 1 and 3). In the general case where both interlayer coupling and anisotropy parameter are present, the situation is more complicated: with increasing temperature the 2D-like Heisenberg behavior changes to the 2D-Ising or 3D-Heisenberg one depending on that anisotropy or interlayer coupling dominate, and finally the system passes to the 3D Ising behavior.

There exist a number of approximations that treat thermodynamics of layered systems. The standard spin-wave theory (SWT) describes satisfactorily the region of rather low temperatures only. Somewhat better results can be obtained by taking into account the temperature renormalization of the interlayer coupling parameter and the anisotropy parameter. The temperature dependence of the anisotropy parameter within the spin-wave theory was considered in Refs. 4–6. A more systematic way to consider such renormalizations is the self-consistent spin-wave theory (SSWT) (Refs. 7 and 8), which was applied to quasi-2D and anisotropic 2D magnets in Refs. 9–12.

SSWT takes into account the interaction between spin waves in the lowest Born approximation. However, at not too low temperatures this approximation is insufficient. In particular, the values of the ordering temperature in SSWT are still too high in comparison with experimental ones, and the critical behavior is quite incorrect. Thus the summation of leading contributions in all orders of perturbation theory should be performed. At the same time, to describe the behavior of the order parameter in the critical region one has to take into consideration fluctuation (non-spin-wave) contribution to thermodynamic quantities. Ising-like excitations in a classical anisotropic model were considered in Ref. 13. At the same time, in the quantum anisotropic case this treatment meets with difficulties,[14] and 3D fluctuations in the critical region of quasi-2D magnets cannot be considered in the approach[13,14] too.

A possible way to sum up an infinite sequence of perturbation contributions is the renormalization group (RG) analysis. The RG approach was successfully used to consider the classical isotropic magnets with the space dimensionality $d=2$ (Ref. 15) and $d=2+\varepsilon$.[16,17] In the latter case the renormalized coupling constant at the fixed point is small (of order of ε), and the standard technique of the ε expansion can be applied. Physically, this means that the excitation-spectrum picture differs somewhat from the spin-wave one (as discussed in Ref. 3, the fluctuation corrections to the excitation spectrum read $\delta E_{\mathbf{q}} \sim \varepsilon \ln q$). The RG method was applied also to quantum 2D isotropic magnets in Ref. 18.

The scaling behavior in the quasi-2D or anisotropic 2D systems is expected to differ from the isotropic $d=2+\varepsilon$ magnet. In these cases the renormalized value of the coupling constant at the stability point of the RG transformation is not small, which corresponds to above-discussed crossover from the 2D-like Heisenberg to 3D Heisenberg (or 2D Ising) critical regime. Thus the RG method does not work when passing to the true critical region. The latter region should be considered with account of essentially non-spin-wave (fluctuation) excitations.

To take into account non-spin-wave effects it is convenient to use, instead of the original Heisenberg model, models with large degeneracy, which enables one to introduce a formal small parameter in the theory. In Ref. 3 an isotropic quantum quasi-2D antiferromagnet was investigated within

the $1/N$ expansion in the quantum $O(N)$ model[19] (in the Heisenberg model, $N=3$). It was demonstrated that the renormalizations of the interlayer coupling parameter in comparison with the usual spin-wave theory (and also SSWT) determine considerable lowering of the transition point. The same situation should be expected for 2D anisotropic magnets. At the same time, the $1/N$ expansion meets with some difficulties at the description of the 2D-like region where the series expansion is performed in powers of $1/(N-2)$ rather than $1/N$.[19,3]

Thus the RG approach and $1/N$ expansion in the $O(N)$ model are expected to have advantages in different temperature regions. Whereas the first method describes well the 2D-like regime, the $1/N$ expansion treats satisfactorily the critical region. An advantage of the RG approach in comparison with the technique of the $1/N$ expansion in the $O(N)$ model is that it enables one to consider the quantum ferromagnet case where the partition function cannot be generalized to arbitrary N. The RG analysis permits also to treat the classical case, which is difficult within the $1/N$ expansion. (In the classical case, there is no natural upper cutoff for quasimomenta, which is the temperature in the quantum case, and the original lattice version of the partition function should be considered.)

The Heisenberg model can be also considered as a particular case of the $SU(M)$ model (or of its continuum analog, CP^{M-1} model) with $M=2$ (see, e.g., Ref. 20). Since the $M\to\infty$ limit corresponds to SSWT (see, e.g., Ref. 8), at finite M thermodynamics is described in terms of spin-wave picture of the excitation spectrum. The corresponding $1/M$-expansion contains in the 2D case infrared-divergent terms[21] and is rather inconvenient. For d not close to 2, this expansion does not enable one to obtain correct values of the critical exponents.[22] Thus, as well as in RG approach, only the 2D-like isotropic Heisenberg region can be considered within the $1/M$ expansion. Furthermore, the results of CP^{M-1} model to nth order in $1/M$ are expected to coincide at $M=2$ with the $(n+1)$-loop RG analysis for $O(3)$ or, equivalently, CP^1 model (we do not know a general proof of this statement, but this is true in the $d=2+\varepsilon$ case for $n=0,1$; see Ref. 22).

The simplest one-loop RG analysis was applied earlier to calculation of the Curie temperature of anisotropic 2D ferromagnets.[23] As we shall see below, the results of this work become considerably modified by the two-loop corrections, which were not taken into account in Ref. 23. The momentum-shell version of the one-loop RG approach in the classical quasi-2D magnets was considered in Ref. 24. However, the authors of this paper passed to continuum limit in the direction perpendicular to layers, so that results of Ref. 24 at small interlayer coupling have qualitative rather than quantitative character.

In the present paper we consider thermodynamics of the quantum and classical layered magnets with small interlayer coupling and anisotropy within the consistent two-loop RG approach and first-order $1/N$ expansion in the $O(N)$ model.

The plan of the paper is as follows. In Sec. II we consider the continuum and lattice versions of the $O(N)$ model for anisotropic layered ferromagnets and antiferromagnets. In Sec. III we apply the renormalization-group approach[16,18] to the quantum $O(N)$ model in the (isotropic) 2D-like region (the classical case is considered in Appendix B). In Sec. IV we investigate the same problem within the $1/N$ expansion in the $O(N)$ model up to the first order and treat the crossover from the 2D-like to 3D Heisenberg (or 2D Ising) behavior. In Sec. V we summarize our results and compare them with experimental data on layered antiferromagnets.

II. CONTINUUM AND LATTICE MODELS FOR THE SPIN SYSTEM

We consider the Heisenberg model with small interlayer coupling and easy-axis anisotropy,

$$H=-\frac{J}{2}\sum_{i\delta_\parallel}\mathbf{S}_i\mathbf{S}_{i+\delta_\parallel}+H_{3\mathrm{D}}+H_{\mathrm{anis}}, \tag{1}$$

$$H_{3\mathrm{D}}=-\frac{\alpha J}{4}\sum_{i\delta_\perp}\mathbf{S}_i\mathbf{S}_{i+\delta_\perp}, \tag{2}$$

$$H_{\mathrm{anis}}=-\frac{J\eta}{2}\sum_{i\delta_\parallel}S_i^zS_{i+\delta_\parallel}^z-|J|\zeta\sum_i(S_i^z)^2, \tag{3}$$

where $J>0$ for a ferromagnet, $J<0$ for an antiferromagnet, $\delta_\parallel$ and $\delta_\perp$ denote nearest neighbors within a layer and for different layers, $\alpha>0$ is the interlayer coupling parameter, and $\eta,\zeta>0$ are the parameters of the exchange anisotropy and single-site anisotropy, respectively. The partition function of the model (1) can be represented in terms of a path integral over coherent states (see, e.g., Refs. 25 and 8):

$$\mathcal{Z}=\int D\mathbf{n}D\lambda\exp\left\{\frac{JS^2}{2}\int_0^{1/T}d\tau\sum_i\left[\frac{2\mathrm{i}}{JS}\mathbf{A}(\mathbf{n}_i)\frac{\partial\mathbf{n}_i}{\partial\tau}+\mathbf{n}_i\mathbf{n}_{i+\delta_\parallel}+\frac{\alpha}{2}\mathbf{n}_i\mathbf{n}_{i+\delta_\perp}+\eta n_i^zn_{i+\delta_\parallel}^z+\mathrm{sgn}(J)\tilde{\zeta}(n_i^z)^2+hn_i^z+\mathrm{i}\lambda_i(\mathbf{n}_i^2-1)\right]\right\} \tag{4}$$

with $\mathbf{n}_i(\tau)$ the three-component unit-length vector field, $\mathbf{A}(\mathbf{n})$ the vector potential of the unit magnetic monopole, which satisfies the equation $\boldsymbol{\nabla}\times\mathbf{A}(\mathbf{n})\cdot\mathbf{n}=1$, $\tilde{\zeta}=2\zeta(1-1/2S)$ and the summation over $\delta_\parallel,\delta_\perp$ in Eq. (4) is assumed. We have also introduced in Eq. (4) the external magnetic field h to perform the calculation of spin correlation functions. The term with the time derivative corresponds to the Berry-phase contribution.[26] Depending on the value of T/JS, two cases are possible: (a) the classical case $T\gg JS$ and (b) the quantum case $T\ll JS$.

Consider first the classical case. The main contribution to Eq. (4) comes from time-independent paths, and the partition function reduces to

$$\mathcal{Z}_{\rm cl}=\int D\mathbf{n}D\lambda\exp\left\{\frac{\rho_s^0}{2T}\sum_i\left[\mathbf{n}_i\mathbf{n}_{i+\delta_\parallel}+\frac{\alpha}{2}\mathbf{n}_i\mathbf{n}_{i+\delta_\perp}+\eta n_i^z n_{i+\delta_\parallel}^z+\tilde{\zeta}(n_i^z)^2+hn_i^z+i\lambda(\mathbf{n}_i^2-1)\right]\right\} \tag{5}$$

with $\rho_s^0=|J|S^2$ the bare spin stiffness. To derive Eq. (5) in the antiferromagnetic case we have replaced $\mathbf{n}_i\to-\mathbf{n}_i,\lambda_i\to-\lambda_i$ at one of two sublattices. Thus in the classical case the results for $\mathcal{Z}$ are identical for a ferromagnet and antiferromagnet. In the continuum limit the partition function (5) coincides with that of the well-known classical nonlinear-σ model.[8] However, if one is interested in thermodynamics in a wide temperature interval (not only in the critical region), the continuum limit cannot be used since not only long-wave excitations contribute thermodynamic properties.

Now we treat the quantum case. Then the temperature plays the role of a natural upper limit cutoff for frequencies of the fluctuations. Thus we may pass to the continuum limit within each layer. For a ferromagnet we use the representation

$$\mathbf{A}(\mathbf{n})=\frac{\mathbf{z}\times\mathbf{n}}{1+(\mathbf{zn})} \tag{6}$$

($\mathbf{z}$ is the unit vector along the z axis). Then we obtain

$$\mathcal{Z}_{\rm F}=\int\frac{D\boldsymbol{\pi}}{\sqrt{1-\boldsymbol{\pi}^2}}\exp\left\{-\frac{\rho_s^0}{2}\int_0^{1/T}d\tau\int d^2\mathbf{r}\times\sum_{i_z}\left[\frac{2i}{JS}\frac{1-\sqrt{1-\boldsymbol{\pi}_{i_z}^2}}{\boldsymbol{\pi}_{i_z}^2}\left(\pi_{i_z}^x\frac{\partial\pi_{i_z}^y}{\partial\tau}-\pi_{i_z}^y\frac{\partial\pi_{i_z}^x}{\partial\tau}\right)+(\nabla\boldsymbol{\pi}_{i_z})^2+\frac{\alpha}{2}(\boldsymbol{\pi}_{i_z+1}-\boldsymbol{\pi}_{i_z})^2+(\nabla\sqrt{1-\boldsymbol{\pi}_{i_z}^2})^2+\frac{\alpha}{2}\times(\sqrt{1-\boldsymbol{\pi}_{i_z+1}^2}-\sqrt{1-\boldsymbol{\pi}_{i_z}^2})^2+f\boldsymbol{\pi}_{i_z}^2+h\sqrt{1-\boldsymbol{\pi}_{i_z}^2}\right]\right\}, \tag{7}$$

where i_z is the number of a layer, $\boldsymbol{\pi}=\mathbf{n}-(\mathbf{nz})\mathbf{z}$ is the two-component vector field,

$$f=\tilde{\zeta}+4\eta\equiv 2\zeta(1-1/2S)+4\eta, \tag{8}$$

and we have made the shift $i\lambda\to i\lambda+f$ before integrating over λ.

In the antiferromagnetic quantum case we use the Haldane mapping[26] (see also Ref. 8) to integrate over the ''fast'' components of $\mathbf{n}$. Thus we pass to the partition function of the quantum nonlinear σ model

$$\mathcal{Z}_{\rm AF}=\int D\boldsymbol{\sigma}D\lambda\exp\left\{-\frac{\rho_s^0}{2}\int_0^{1/T}d\tau\int d^2\mathbf{r}\times\sum_{i_z}\left[\frac{1}{c_0^2}(\partial_\tau\boldsymbol{\sigma}_{i_z})^2+(\nabla\boldsymbol{\sigma}_{i_z})^2+\frac{\alpha}{2}(\boldsymbol{\sigma}_{i_z+1}-\boldsymbol{\sigma}_{i_z})^2 \right.\right. \tag{9}$$

$$\left.\left.-f(\sigma_{i_z}^z)^2+h\sigma_{i_z}^z+i\lambda(\boldsymbol{\sigma}_{i_z}^2-1)\right]\right\}, \tag{10}$$

where $\boldsymbol{\sigma}_{i_z}$ is the three-component unit-length field and $c_0=\sqrt{8}JS$ is the bare spin-wave velocity. Unlike the quantum ferromagnet case, this model can be trivially extended to the $O(N)$ symmetry with arbitrary N, the N-component vector field $\sigma_i=\{\sigma_1\ldots\sigma_N\}$ being introduced and σ^z being replaced by σ_N. Writing down $\sigma=\{\pi_1\ldots\pi_{N-1},\sigma_N\}$ we have

$$\mathcal{Z}_{\rm AF}=\int\frac{D\boldsymbol{\pi}}{\sqrt{1-\boldsymbol{\pi}^2}}\exp\left\{-\frac{\rho_s^0}{2}\int_0^{1/T}d\tau\int d^2\mathbf{r}\sum_{i_z}\left[(\partial_\mu\boldsymbol{\pi}_{i_z})^2+(\partial_\mu\sqrt{1-\boldsymbol{\pi}_{i_z}^2})^2+\frac{\alpha}{2}(\boldsymbol{\pi}_{i_z+1}-\boldsymbol{\pi}_{i_z})^2+f\boldsymbol{\pi}^2+\frac{\alpha}{2}(\sqrt{1-\boldsymbol{\pi}_{i_z+1}^2}-\sqrt{1-\boldsymbol{\pi}_{i_z}^2})^2+h\sqrt{1-\boldsymbol{\pi}_{i_z}^2}\right]\right\}, \tag{11}$$

where $\partial_\mu=[\partial/\partial(c_0\tau),\nabla]$, and we have performed the shift $i\lambda\to i\lambda+f$.

III. RENORMALIZATION-GROUP ANALYSIS IN THE 2D-LIKE REGIME FOR THE QUANTUM CASE

Using the above expressions for the partition function we can develop a scaling approach. We use the field theory formulation of RG transformation.[28,16] To develop this approach we pass to the renormalized theory with the use of the relations[16]

$$\begin{aligned} g&=g_RZ_1,\quad u=u_RZ_u\\ \pi&=\pi_RZ,\quad h=h_RZ_1/\sqrt{Z}\\ f&=f_RZ_2,\quad \alpha=\alpha_RZ_3, \end{aligned} \tag{12}$$

where the index R corresponds to the renormalized quantities, the bare coupling constant g, and the dimensionless inverse temperature u are determined by

$$g=1/S,\quad u=JS/T\quad\text{(FM)} \tag{13}$$

$$g=c_0/\rho_s^0,\quad u=c_0/T\quad\text{(AFM)}. \tag{14}$$

The renormalization constants Z_i are chosen from the condition that the thermodynamic quantities are independent of an upper cutoff. Since the nonlinear-σ model is renormalizable (see Ref. 28), five renormalization constants for five independent parameters of the model are sufficient to this end. To calculate renormalization constants it is sufficient to calculate the renormalization of the one-particle Green's function in an external magnetic field.[28,16]

Consider first the case of an antiferromagnet. The perturbation theory in the coupling constant for the partition function (11) can be developed in a standard way.[16–18] After expanding the square roots in a series in the field π, the bare Green's function of this field takes the form

$$G^{(0)}(\mathbf{p},i\omega_n)=\frac{1}{g}[\omega_n^2+p_\parallel^2+\alpha(1-\cos p_z)+f+h]^{-1}, \tag{15}$$

where $p_\parallel=(p_x^2+p_y^2)^{1/2}$, $\omega_n=2\pi n/u$ are the dimensionless Matsubara frequencies. In each order of perturbation theory

one has to take into account all the possible connected diagrams with the fixed number of loops.

We consider only the ''renormalized classical'' regime

$$T \gg (\max\{f,\alpha\})^{1/2} c, \tag{16}$$

since in the interval $T < (\max\{f,\alpha\})^{1/2} c$ the staggered magnetization is well described by SSWT (see a more detailed discussion of different temperature regimes in Ref. 3). Since in this regime the quasimomentum cutoff parameter for quantum fluctuations is the boundary of the Brillouin zone Λ, while for thermal ones this is T/c, effects of quantum and thermal fluctuations can be separated (see, e.g., Refs. 19 and 3). Thus it is useful to perform the renormalization in two steps. At the first step the ground-state quantum renormalizations are performed, and the second step is the temperature renormalization. To this end we represent the renormalization constants as

$$Z_i(g,u,\Lambda) = Z_{Qi}(g,\Lambda)\widetilde{Z}_i(g_r,u_r), \tag{17}$$

where $Z_{Qi}(g)$ contain ground-state quantum renormalizations, and $\widetilde{Z}_i$ all the others, and

$$g_r = Z_{Q1}^{-1} g, \quad u_r = Z_{Qu}^{-1} u \tag{18}$$

are the quantum-renormalized coupling constant and dimensionless inverse temperature, respectively. Note that the latter is renormalized due to the renormalization of the spin-wave velocity, $c = Z_{Qu} c_0$. For further convenience we also introduce the quantum-renormalized anisotropy and interlayer coupling parameters,

$$f_r = Z_{Q2}^{-1} f, \quad \alpha_r = Z_{Q3}^{-1} \alpha, \tag{19}$$

which are just experimentally observed. Up to one-loop order we have

$$Z_Q = 1 - (N-1)\frac{g\Lambda}{4\pi} + \mathcal{O}(g^2)$$

$$Z_{Q1} = 1 - (N-2)\frac{g\Lambda}{4\pi} + \mathcal{O}(g^2), \quad Z_{Qu} = 1 + \mathcal{O}(g^2) \tag{20}$$

$$Z_{Q2} = 1 + \frac{g\Lambda}{2\pi} + \mathcal{O}(g^2), \quad Z_{Q3} = 1 + \frac{3g\Lambda}{4\pi} + \mathcal{O}(g^2).$$

Since the renormalization constants Z_{Qi} are nonuniversal, the continuum limit is insufficient to calculate them, and quantum-renormalized parameters can be determined only from the consideration of the original lattice partition function (4) in the ground state. For the square-lattice antiferromagnet this can be performed within the spin-wave theory, which is in fact a series expansion in g ($g \sim 1/S$). The results of the spin-wave theory are presented in Appendix A. We have to first order in $1/S$,

$$Z_Q = 1/Z_{Q1} = Z_{Q2} = Z_{Q3}^{1/2} = 1 - 0.197/S,$$

$$Z_{Qu} = 1 + 0.079/S. \tag{21}$$

After performing the ground-state quantum renormalizations (20) in the continuum model [or, equivalently, renormalizations (21) in the original lattice model] the theory becomes completely universal, i.e., thermodynamic properties do not depend on the cutoff parameter Λ.

Now we pass to the consideration of the temperature renormalizations. The calculation of the renormalization constants $\widetilde{Z}_i$ is performed in the same way as in Ref. 16 and leads to $\widetilde{Z}_u \equiv 1$,

$$\widetilde{Z} = 1 + t_r(N-1)\ln(u_r\mu) + t_r^2(N-1)(N-3/2)\ln^2(u_r\mu) + \mathcal{O}(t_r^3),$$

$$\widetilde{Z}_1 = 1 + t_r(N-2)\ln(u_r\mu) + t_r^2(N-2)\ln^2(u_r\mu) + \mathcal{O}(t_r^3),$$

$$\widetilde{Z}_2 = 1 - 2t_r\ln(u_r\mu) + \mathcal{O}(t_r^2),$$

$$\widetilde{Z}_3 = 1 - t_r\ln(u_r\mu) + \mathcal{O}(t_r^2), \tag{22}$$

where μ is an infrared cutoff parameter with the dimensionality of the inverse length and $t_r = g_r/(2\pi u_r)$. The only difference from the results of Ref. 16 is that the ultraviolet cutoff parameter in Eq. (22) is u_r (rather than Λ in the classical case), and two new renormalization constants, $\widetilde{Z}_2$ and $\widetilde{Z}_3$, for the anisotropy and interlayer coupling parameters occur.

The infinitesimal change of μ generates the renormalization group transformation, and the derivatives of Z factors with respect to μ determine the renormalized-parameters flow functions (see, e.g., Ref. 28). Since quantum-renormalization constants (20) are invariant under RG transformation, it is sufficient to calculate the derivatives of $\widetilde{Z}$. To the two-loop order we have (cf. Refs. 16 and 28)

$$\beta(t_r) \equiv \mu\frac{dt_r}{d\mu} = -(N-2)t_r^2 - (N-2)t_r^3 + \mathcal{O}(t_r^4), \tag{23}$$

$$\mathfrak{s}(t_r) \equiv \mu\frac{d\ln Z}{d\mu} = (N-1)t_r + \mathcal{O}(t_r^3) \tag{24}$$

(to one-loop order, these expressions were obtained earlier by Polyakov[15]).

The flow functions for the interlayer coupling and anisotropy parameters will be needed only to the one-loop approximation:

$$\gamma_f(t_r) \equiv \mu\frac{d\ln Z_2}{d\mu} = -2t_r + \mathcal{O}(t_r^2), \tag{25}$$

$$\gamma_\alpha(t_r) \equiv \mu\frac{d\ln Z_3}{d\mu} = -t_r + \mathcal{O}(t_r^2). \tag{26}$$

Using Eqs. (23)–(26) we find the scaling laws for the Hamiltonian parameters under RG transformation. The equations for the coupling constant t_ρ and renormalization factor Z_ρ at the scale $\mu\rho$ are well known:[16]

$$\rho = \exp\left[\int_{t_r}^{t_\rho}\frac{dt}{\beta(t)}\right] = \left(\frac{t_\rho}{t_r}\right)^{1/(N-2)} \exp\left[\frac{1}{N-2}\left(\frac{1}{t_\rho} - \frac{1}{t_r}\right)\right] \times [1 + \mathcal{O}(t_\rho)], \tag{27}$$

$$Z_\rho=\exp\left[-\int_{t_r}^{t_\rho}\frac{s(t)}{\beta(t)}dt\right]$$
$$=\left(\frac{t_\rho}{t_r}\right)^{(N-1)/(N-2)}\left[1+\frac{N-1}{N-2}(t_r-t_\rho)+\mathcal{O}(t_\rho^2)\right]. \quad (28)$$

The expressions for the effective-anisotropy and interlayer coupling parameters f_ρ,α_ρ at the scale $\mu\rho$ have the form

$$f_\rho=f_r\exp\left[-\int_{t_r}^{t_\rho}\frac{\gamma_f(t)}{\beta(t)}dt\right]=f_r\left(\frac{t_\rho}{t_r}\right)^{-2/(N-2)}[1+\mathcal{O}(t_\rho)], \quad (29)$$

$$\alpha_\rho=\alpha_r\exp\left[-\int_{t_r}^{t_\rho}\frac{\gamma_\alpha(t)}{\beta(t)}dt\right]=\alpha_r\left(\frac{t_\rho}{t_r}\right)^{-1/(N-2)}[1+\mathcal{O}(t_\rho)]. \quad (30)$$

Now we are ready to calculate the relative sublattice magnetization $\bar{\sigma}_r=\bar{\sigma}/\bar{\sigma}_0$, where $\bar{\sigma}=\bar{S}/S$ ($\bar{S}=\langle S^z_{\mathbf{Q}}\rangle$ is the staggered magnetization) and $\bar{\sigma}_0\equiv\bar{\sigma}(T=0)$. The perturbation result in the zero magnetic field up to terms of the order of t_r^2 reads

$$\bar{\sigma}_r=1-\frac{t_r(N-1)}{4}\ln\frac{2}{u_r^2\Delta(f_r,\alpha_r)}+\frac{t_r^2(3-N)(N-1)}{32}\ln^2\frac{2}{u_r^2\Delta(f_r,\alpha_r)}-\frac{t_r^2(N-1)(B_2-2)}{8}\ln\frac{2}{u_r^2\Delta(f_r,\alpha_r)}, \quad (31)$$

where

$$\Delta(f,\alpha)=f+\alpha+\sqrt{f^2+2\alpha f}, \quad (32)$$

$$B_2=3+f_r/\sqrt{f_r^2+2\alpha_r f_r}. \quad (33)$$

Note that the last term in Eq. (31) corresponds to temperature renormalizations of the interlayer coupling and anisotropy parameters:

$$\tilde{f}_r=f_r\left[1-t_r\ln\frac{2}{u_r^2\Delta(f_r,\alpha_r)}\right], \quad (34)$$

$$\tilde{\alpha}_r=\alpha_r\left[1-\frac{t_r}{2}\ln\frac{2}{u_r^2\Delta(f_r,\alpha_r)}\right]. \quad (35)$$

Within the RG approach we obtain from Eq. (28) the following scaling law for the sublattice magnetization:

$$\bar{\sigma}_r(t_r,f_r,\alpha_r,\mu_r)=Z_\rho^{-1/2}\bar{\sigma}_r(t_\rho,f_\rho,\alpha_\rho,\mu\rho), \quad (36)$$

or, equivalently,

$$\frac{\bar{\sigma}_r(t_r,f_r,\alpha_r,\mu)}{\bar{\sigma}_r(t_\rho,f_\rho,\alpha_\rho,\mu\rho)}=\left(\frac{t_r}{t_\rho}\right)^{\beta_2}[1-\beta_2(t_r-t_\rho)+\mathcal{O}(t_\rho^2)], \quad (37)$$

where

$$\beta_2=\frac{N-1}{2(N-2)} \quad (38)$$

is the sublattice-magnetization ''critical exponent'' in the temperature interval under consideration. This coincides with the $\varepsilon\to 0$ limit of the critical exponent $\beta_{2+\varepsilon}$ for $d=2+\varepsilon$ (Ref. 16). The equation for t_ρ/t_r is given by Eq. (27), which can be rewritten as

$$\frac{t_r}{t_\rho}=1+t_r\ln\left(\frac{t_r}{t_\rho}\rho^{N-2}\right)+t_r\mathcal{O}(t_\rho). \quad (39)$$

Finally, the scale ρ is fixed by the condition that the arguments of logarithms in Eq. (31) on this scale are equal to unity, i.e., by $\bar{\sigma}_r(t_\rho,f_\rho,\alpha_\rho,\mu\rho)=1$. Taking into account that u scales in a trivial way, $u_\rho=u_r/\rho$, we obtain the additional equation for ρ:

$$2\rho^2=u_r^2\Delta(f_\rho,\alpha_\rho) \quad (40)$$

We have from Eqs. (37), (39), (29), (30), and (40) the equation for the relative sublattice magnetization in the two-loop RG analysis,

$$\bar{\sigma}_r^{1/\beta_2}=1-\frac{t_r}{2}\left[(N-2)\ln\frac{2}{u_r^2\Delta(f_t,\alpha_t)}+\frac{2}{\beta_2}\ln(1/\bar{\sigma}_r)+2(1-\bar{\sigma}_r^{1/\beta_2})+\mathcal{O}(t_r/\bar{\sigma}_r^{1/\beta_2})\right], \quad (41)$$

where f_t and α_t are the temperature-renormalized parameters of the anisotropy and interlayer coupling. We derive for these quantities

$$f_t/f_r=\bar{\sigma}_r^{4/(N-1)}[1+\mathcal{O}(t_r/\bar{\sigma}_r^{1/\beta_2})], \quad (42)$$

$$\alpha_t/\alpha_r=\bar{\sigma}_r^{2/(N-1)}[1+\mathcal{O}(t_r/\bar{\sigma}_r^{1/\beta_2})]. \quad (43)$$

The leading logarithmic term in the square brackets of Eq. (41) corresponds to SSWT, while the other two terms describe corrections to this theory. As it should be expected, at low temperatures the RG results Eqs. (41), (42), and (43) reduce to corresponding perturbation expressions (31), (34), and (35). We have to bear in mind that the quantity $t_r/\bar{\sigma}_r^{1/\beta_2}$ is a formal rather than real estimate for neglected terms since higher order terms also yield a contribution at not too low temperatures. Physically, neglecting such terms is equivalent to neglecting 3D (or Ising-like) fluctuations in the RG approach.

As already pointed out, the Néel temperature cannot be calculated directly in the RG approach since essentially non-spin-wave fluctuations contribute to it and a consideration of diagrams with an arbitrary number of loops is required. However, one can obtain a general expression for the Néel temperature in the following way. Consider first the temperature t_r^* of the crossover to the true critical region. This is determined by the condition $t_\rho\sim 1$, i.e., $t_r^*\sim\bar{\sigma}_r^{1/\beta_2}$ [the scale ρ is determined by Eq. (40)]. Substituting this into Eq. (41) one obtains

$$t_r^*=2\Big/\left[(N-2)\ln\frac{2}{u_r^2\Delta(f^*,\alpha^*)}+2\ln(2/t_r^*)+C_{\rm AF}\right], \tag{44}$$

where $f^*=f_r(t_r^*)^{2/(N-2)}$, $\alpha^*=\alpha_r(t_r^*)^{1/(N-2)}$, and $C_{\rm AF}$ is some constant of order of unity. With further flow of RG parameters, 3D Heisenberg (or 2D Ising) fluctuations change only the constant $C_{\rm AF}$ which is replaced by the universal function $\Phi_{\rm AF}(\alpha_r/f_r)\sim 1$. Thus for the Néel temperature we have

$$t_{\rm Néel}=2\Big/\left[(N-2)\ln\frac{2}{u_r^2\Delta(f_c,\alpha_c)}+2\ln(2/t_{\rm Néel})+\Phi_{\rm AF}(\alpha_r/f_r)\right], \tag{45}$$

where

$$f_c=f_r t_{\rm Néel}^{2/(N-2)},\quad \alpha_c=\alpha_r t_{\rm Néel}^{1/(N-2)} \tag{46}$$

[recall that $t=T/(2\pi\rho_s)$, $u_r=c/T$]. The function Φ is determined by non-spin-wave fluctuations and cannot be calculated within the RG approach. Note that the equation (45) is analogous to the result for the correlation length in the renormalized classical regime in the 2D case,[18,19] which may be rewritten in the same manner:

$$t_r=2/[(N-2)\ln(\xi^2/u_r^2)+2\ln(2/t_r)+\ln C_\xi], \tag{47}$$

where C_ξ is an universal numerical preexponential factor. Comparing Eqs. (45) and (47) we see that the only difference is that in the quasi-2D anisotropic case the logarithms are cut at $\Delta^{1/2}$ (rather than at $1/\xi$ in the isotropic 2D case). In the quasi-2D isotropic case the quantity Φ can be calculated within the $1/N$ expansion (see the next section), and a more general case requires numerical analysis (e.g., the quantum Monte Carlo method).

Three limiting cases may be considered.

(i) The anisotropic 2D case $\alpha=0$. The equation for magnetization (41) takes the form

$$\bar\sigma_r^{1/\beta_2}=1-\frac{t_r}{2}\left[(N-2)\ln\frac{1}{u_r^2 f_r}+\frac{4}{\beta_2}\ln(1/\bar\sigma_r)+2(1-\bar\sigma_r^{1/\beta_2})+\mathcal{O}(t_r/\bar\sigma_r^{1/\beta_2})\right]. \tag{48}$$

The equation for the Néel temperature (45) reads

$$t_{\rm Néel}=2\Big/\left[(N-2)\ln\frac{1}{u_r^2 f_r}+4\ln(2/t_{\rm Néel})+\Phi_{\rm AF}(\infty)\right]. \tag{49}$$

(ii) The isotropic quasi-2D case $f=0$. We obtain

$$\bar\sigma_r^{1/\beta_2}=1-\frac{t_r}{2}\left[(N-2)\ln\frac{2}{u_r^2\alpha_r}+\frac{3}{\beta_2}\ln(1/\bar\sigma_r)+2(1-\bar\sigma_r^{1/\beta_2})+\mathcal{O}(t_r/\bar\sigma_r^{1/\beta_2})\right], \tag{50}$$

$$t_{\rm Néel}=2\Big/\left[(N-2)\ln\frac{2}{u_r^2\alpha_r}+3\ln(2/t_{\rm Néel})+\Phi_{\rm AF}(0)\right]. \tag{51}$$

(iii) The large-N case. To retain the structure of the equation (40) at finite N, it is convenient to expand Eq. (40) in $1/(N-2)$ rather than in $1/N$. To first order we obtain

$$\rho^2\simeq\frac{\Delta(f_r,\alpha_r)}{2}\left[1+\frac{B_2-2}{N-2}\ln\frac{t_r}{t_\rho}\right]\simeq\frac{\Delta(f_r,\alpha_r)}{2}\left(\frac{t_r}{t_\rho}\right)^{(B_2-2)/(N-2)}. \tag{52}$$

Then we have

$$\bar\sigma_r^{1/\beta_2}=1-\frac{t_r}{2}\left[(N-2)\ln\frac{2}{u_r^2\Delta(f_r,\alpha_r)}+B_2\ln(1/\bar\sigma_r^2)+2(1-\bar\sigma_r^2)+\mathcal{O}(t_r/\bar\sigma_r^2,1/N)\right] \tag{53}$$

and

$$t_{\rm Néel}=2\Big/\left[(N-2)\ln\frac{2}{u_r^2\Delta(f_r,\alpha_r)}+B_2\ln(2/t_{\rm Néel})+\Phi_{\rm AF}(\alpha_r/f_r)\right]. \tag{54}$$

The ferromagnetic case can be considered in a similar way. In this case the quantum ground-state renormalizations are absent and the ''classical'' regime (an analogue of the ''renormalized classical'' one in the antiferromagnetic case) is determined by

$$T\gg JS\max\{f,\alpha\}. \tag{55}$$

To develop perturbation theory for the partition function (7) we pass from the real fields π_x,π_y to the cyclic components

$$\pi^\pm=\pi_x\pm i\pi_y \tag{56}$$

and expand again square roots in π^+,π^-. The bare Green's function of the fields π^+,π^- takes the form

$$G^{(0)}(\mathbf{p},i\omega_n)=\frac{1}{g}[i\omega_n+p_\parallel^2+\alpha(1-\cos p_z)+f+h]^{-1}. \tag{57}$$

Due to absence of quantum renormalizations we have $Z_{Qi}\equiv 1$ and the indices r may be dropped. The factors $\tilde{Z}_i$ has the same form (22) as in the antiferromagnetic case with $N=3$ and the replacement $\ln(u_r\mu)\to\ln(u\mu)/2$.

The relative magnetization $\bar{\sigma}\equiv\overline{S}/S$ ($\overline{S}=\langle S^z\rangle$) to the two-loop approximation reads

$$\bar{\sigma}=1-\frac{t}{2}\ln\frac{2}{u\Delta(f,\alpha)}-\frac{t^2}{4}(B_2-2)\ln\frac{2}{u\Delta(f,\alpha)} \tag{58}$$

($t=g/u$). The scaling equation (37) is valid in the ferromagnetic case too. The equation for ρ in this case takes the form

$$2\rho^2=u\Delta(f_\rho,\alpha_\rho). \tag{59}$$

Thus we obtain the equation for the magnetization in the form

$$\bar{\sigma}=1-\frac{t}{2}\left[\ln\frac{2}{u\Delta(f_t,\alpha_t)}+2\ln(1/\bar{\sigma})+2(1-\bar{\sigma})+\mathcal{O}(t/\bar{\sigma})\right]. \tag{60}$$

The results for the temperature renormalization of the anisotropy and interlayer coupling parameters have the same form (42), (43). The Curie temperature is determined in the same way as the Néel temperature in the antiferromagnetic case. The result reads

$$t_{\mathrm{Curie}}=2\Big/\left[\ln\frac{2}{u\Delta(f_c,\alpha_c)}+2\ln(2/t_{\mathrm{Curie}})+\Phi_{\mathrm{F}}(\alpha/f)\right]. \tag{61}$$

The calculation of the magnetization and ordering temperature of a classical magnet is performed in Appendix B.

Thus the RG approach is sufficient to calculate the magnetization in the spin-wave and the 2D-like regions and to calculate the Néel (Curie) temperature up to some universal constant. The crossover temperature region of the quantum antiferromagnet can be considered within the $1/N$ expansion. Besides that, in the case of quantum quasi-2D antiferromagnet, this expansion enables one to describe the true critical region and to evaluate the quantity $\Phi_{\mathrm{AF}}(0)$.

IV. COMPARISON WITH THE $1/N$ EXPANSION IN THE QUANTUM $O(N)$ MODEL AND THE CROSSOVER TO THE CRITICAL REGIME

The $1/N$ expansion gives a possibility to develop another perturbation theory for the partition function (11). Unlike the renormalization group approach, this method works satisfactorily at arbitrary temperatures. As well as in Sec. III, we consider only the ordered phase.

Consider first the case of the antiferromagnet. We begin with the generalization of the results of Ref. 3 to the case where anisotropy is present. To develop perturbation theory in $1/N$ we integrate out σ fields from Eq. (11). Thus we have

$$\mathcal{Z}_{\mathrm{AF}}=\int D\lambda\exp(NS_{\mathrm{eff}}[\lambda,h]) \tag{62}$$

$$S_{\mathrm{eff}}[\lambda,h]=\frac{1}{2}\ln\,\det\hat{G}_0+\frac{1}{2g}(1-\overline{\sigma^2})\mathrm{Sp}(i\lambda)+\frac{1}{2g}\mathrm{Sp}[(i\lambda\bar{\sigma}-h/\rho_s^0)\hat{G}_0(i\lambda\bar{\sigma}-h/\rho_s^0)], \tag{63}$$

where

$$\hat{G}_0^{mm}=[\partial_\tau^2+\nabla^2+\alpha\Delta_z+f(1-\delta_{mN})]^{-1},$$
$$\Delta_z\sigma_{i_z}(\mathbf{r},\tau)=\sigma_{i_z+1}(\mathbf{r},\tau)-\sigma_{i_z}(\mathbf{r},\tau) \tag{64}$$

and $\bar{\sigma}=\langle\sigma_N(\mathbf{r},\tau)\rangle$ is the relative staggered magnetization.

Since N enters Eq. (62) only as a prefactor in the exponent, expanding near the saddle point generates a series in $1/N$. To zeroth order in $1/N$ the excitation spectrum, which is given by the poles of the unperturbed longitudinal and transverse Green's functions, contains a gap $f^{1/2}$ for all the components σ_m except for $m=N$:

$$G_t^0(\mathbf{q},\omega_n)=[\omega_n^2+q_\parallel^2+\alpha(1-\cos q_z)+f]^{-1} \tag{65}$$

$$G_l^0(\mathbf{q},\omega_n)=[\omega_n^2+q_\parallel^2+\alpha(1-\cos q_z)]^{-1}. \tag{66}$$

The absence of the gap for the Nth (longitudinal) mode in the ordered phase is an *exact* property of the model under consideration in any order in $1/N$.

The sublattice magnetization at $T<T_{\mathrm{Néel}}$ is determined by the constraint equation $\langle\sigma^2\rangle=1$. To first order in $1/N$ the constraint takes the form

$$1-\overline{\sigma^2}=gT\frac{N-1}{N}\sum_{\omega_m}\int\frac{d^2\mathbf{k}_\parallel}{(2\pi)^2}\int_{-\pi}^{\pi}\frac{dk_z}{2\pi}G_t^0(\mathbf{k},\omega_m)+g[F(T,\bar{\sigma})-R(T,\bar{\sigma})], \tag{67}$$

where

$$R(T,\bar{\sigma})=T\sum_{\omega_m}\int\frac{d^2\mathbf{k}_\parallel}{(2\pi)^2}\int_{-\pi}^{\pi}\frac{dk_z}{2\pi}[G_t^0(\mathbf{k},\omega_m)]^2[\Sigma_t(\mathbf{k},\omega_m)-\Sigma_l(\mathbf{0},0)], \tag{68}$$

$$F(T,\bar{\sigma})=\frac{2T}{N}\sum_{\omega_m}\int\frac{d^2\mathbf{k}_\parallel}{(2\pi)^2}\int_{-\pi}^{\pi}\frac{dk_z}{2\pi}G_l^0(\mathbf{k},\omega_m)\frac{\Pi(\mathbf{k},\omega_m)}{\tilde{\Pi}(\mathbf{k},\omega_m)}. \tag{69}$$

The longitudinal and transverse mode self-energies are given by

$$\Sigma_{t,l}(\mathbf{k},\omega_m)=\frac{2T}{N}\sum_{\omega_n}\int\frac{d^2\mathbf{q}_\parallel}{(2\pi)^2}\int_{-\pi}^{\pi}\frac{dq_z}{2\pi}\frac{G_{t,l}^0(\mathbf{k}-\mathbf{q},\omega_m-\omega_n)}{\tilde{\Pi}(\mathbf{q},\omega_n)}, \tag{70}$$

where

$$\tilde{\Pi}(\mathbf{q},\omega_n)=\Pi(\mathbf{q},\omega_n)+\frac{2\bar{\sigma}^2}{g}G_l^0(\mathbf{q},\omega_n), \tag{71}$$

$$\Pi(\mathbf{q},\omega_n)=T\sum_{\omega_l}\int\frac{d^2\mathbf{p}_\parallel}{(2\pi)^2}\int_{-\pi}^{\pi}\frac{dp_z}{2\pi}\Bigg[\frac{N-1}{N}G_t^0(\mathbf{p},\omega_l)\times G_t^0(\mathbf{q}+\mathbf{p},\omega_n+\omega_l)+\frac{1}{N}G_l^0(\mathbf{p},\omega_l)G_l^0(\mathbf{q}+\mathbf{p},\omega_n+\omega_l)\Bigg]. \quad (72)$$

Since the polarization operator $\Pi(q,\omega_n)$ enters only the first-order corrections in Eq. (67), the contribution from longitudinal Green's functions to Π influences thermodynamic quantities in order of $1/N^2$ and can be formally neglected. However, one should bear in mind that for finite N this corrections may be large. Physically, the neglection of the longitudinal part of Π corresponds to neglecting the contribution of Ising-like (spin-flip) excitations. However, these excitations are negligible only at wave vectors $q\gg f^{1/2}$ (see, e.g., Ref. 29). As follows from Eq. (72), such quasimomenta yield a dominant contribution at $T\ll 2\bar{\sigma}^2[(\alpha+f)/f]^{1/2}/g$. The opposite case $T\gg 2\bar{\sigma}^2[(\alpha+f)/f]^{1/2}/g$ corresponds to the Ising critical region, which cannot be treated within the $1/N$ expansion.

As well as in the previous section, we consider only the case $T\gg(\max\{f,\alpha\})^{1/2}c$. The procedure of integration and frequency summation in Eq. (67) is analogous to that of Refs. 19 and 3. We obtain

$$1-\frac{T}{4\pi\rho_s}\Bigg[(N-2)\ln\frac{2T^2}{c^2\Delta}+B_2\ln\frac{\ln(T^2/c^2\Delta)+x_{\bar\sigma}}{x_{\bar\sigma}}-2\frac{\ln(2T^2/c^2\Delta)}{\ln(2T^2/c^2\Delta)+x_{\bar\sigma}}-I_1(x_{\bar\sigma})\Bigg]=\bar{\sigma}_r^2\Bigg[1+\frac{1}{N}\ln\frac{\ln(2T^2/c^2\Delta)+x_{\bar\sigma}}{x_{\bar\sigma}}-I_2(x_{\bar\sigma})\Bigg], \quad (73)$$

where $\Delta\equiv\Delta(f_r,\alpha_r)$ [see Eq. (32)]; B_2 is determined by Eq. (33),

$$x_{\bar\sigma}=\frac{4\pi\rho_s}{(N-2)T}\bar{\sigma}_r^2, \quad (74)$$

and we have introduced the quantum-renormalized parameters

$$f_r=f(1-2Q_\Lambda),\quad \alpha_r=\alpha(1-Q_\Lambda) \quad (75)$$

$$\rho_s=(1+4Q_\Lambda)\rho_s^{N=\infty},\quad \bar{\sigma}_r^2=g\rho_s(1-Q_\Lambda)/N \quad (76)$$

with $\rho_s^{N=\infty}=Nc(1/g-\Lambda/2\pi^2)$ the renormalized spin stiffness in zeroth order in $1/N$, $Q_\Lambda=(8/3\pi^2N)\ln(N\Lambda c/16\rho_s)$ (in this section we use the relativistic cutoff $\omega_n^2+k^2<\Lambda^2$ of frequency summations and quasimomentum integrations; for this regularization scheme the bare spin wave velocity c_0 is replaced by the quantum-renormalized one, c). Since another regularization scheme is used, the expressions (75), (76) are different from the corresponding results of Sec. III. As well as in Sec. III, the quantum-renormalized parameters are not universal and, therefore, should be determined from the spin-wave theory (see Appendix A) rather than from the continuum model. The functions $I_{1,2}(x)$ are some functions with the asymptotics $1/x$ at large x, so that at $x_{\bar\sigma}\gg 1$ their contributions are small. For the isotropic quasi-2D case these functions were calculated in Ref. 3.

Consider first the case of not too high temperatures

$$T(N-2)/4\pi\rho_s<\bar{\sigma}_r^2, \quad (77)$$

where $I_{1,2}(x_{\bar\sigma})$ are small enough. Using the identity $\ln(T^2/c^2\Delta)+x_{\bar\sigma}=4\pi\rho_s/(N-2)T$, which holds to zeroth order in $1/N$, we transform the logarithmic term in the right-hand side of Eq. (73) into a power to obtain

$$[1-I_2(x_{\bar\sigma})]\bar{\sigma}_r^{1/\beta_2}=1-\frac{T}{4\pi\rho_s}\Bigg[(N-2)\ln\frac{2T^2}{c^2\Delta}+B_2\ln(1/\bar{\sigma}_r^2)-2+2\bar{\sigma}_r^2-I_1(x_{\bar\sigma})\Bigg]. \quad (78)$$

Note that in the quasi-2D case ($f=0$) the equation (78) slightly differs from the equation (54) of Ref. 3 by the replacement

$$\ln(2T^2/\alpha_r)/[\ln(2T^2/\alpha_r)+x_{\bar\sigma}]\to 1-\bar{\sigma}_r^2,$$

which leads to errors of order of $1/N^2$.

At temperatures $T(N-2)/4\pi\rho_s\ll\bar{\sigma}_r^2$ the contribution of I_1, I_2 can be neglected and the fluctuations in this temperature region have a 2D-like Heisenberg nature. In particular, in the low-temperature region $T(N-2)\ln(2T^2/\Delta)/4\pi\rho_s\ll\bar{\sigma}_r^2$ the result of SSWT (Refs. 9,11,12),

$$\bar{\sigma}_r=1-\frac{T(N-1)}{8\pi\rho_s}\ln\frac{2T^2}{c^2\Delta}, \quad (79)$$

is reproduced. One can see also that at $I_1=I_2=0$ the result (78) coincides with the large-N limit of the RG result (41) [see Eq. (53)]. However, at finite N the renormalization group provides a more correct description of the sublattice magnetization at $T(N-2)/4\pi\rho_s\ll\bar{\sigma}_r^2$.

In the temperature region $\bar{\sigma}_r^2\sim T(N-2)/4\pi\rho_s$, which corresponds to the crossover to the true critical behavior, the situation changes. In this case the large-N result demonstrates a sharper decrease of $\bar{\sigma}$ than the RG approach. In the quasi-2D case[3] the result (78) is smoothly joined with the 3D temperature dependence (see below). Thus in the quasi-2D case the result of the $1/N$ expansion should be considered as an interpolation between the low-temperature and critical regions. One could expect that this holds also in the presence of the anisotropy where critical behavior cannot be described within the $1/N$ expansion.

In the region $x_{\bar\sigma}\ll 1$, i.e., $\bar{\sigma}_r^2\ll T(N-2)/4\pi\rho_s$, the true critical behavior takes place. In the isotropic quasi-2D case ($f=0$) the result for the staggered magnetization reads (see Ref. 3)

$$\bar{\sigma}_r^2=\Bigg[\frac{4\pi\rho_s}{(N-2)T_{\text{Néel}}}\Bigg]^{\beta_3/\beta_2-1}\Bigg[\frac{1}{1-A_0}\Bigg(1-\frac{T}{T_{\text{Néel}}}\Bigg)\Bigg]^{2\beta_3}, \quad (80)$$

where $\beta_3=(1-8/\pi^2N)/2$ is the true 3D critical exponent for the order parameter (for $N=3$ we have $\beta_3\simeq 0.36$),

$A_0=2.8906/N$. The result of the $1/N$ expansion for $T_{\text{Néel}}$ (Ref. 3) satisfies the general formula (51) with

$$\Phi_{\text{AF}}(0)=-0.0660. \tag{81}$$

In the anisotropic 2D case ($\alpha=0$) the temperature dependence of magnetization in the critical region is determined by the Ising-like excitations (domain walls), which cannot be considered within the $1/N$ expansion. The universality hypothesis predicts the same temperature behavior of $\bar{\sigma}$ as in Ising systems,

$$\bar{\sigma}_r^8=A(1-T/T_{\text{Néel}}), \tag{82}$$

where A is some constant. As numerical calculations demonstrate (see the next section), the temperature dependence of $\bar{\sigma}$ determined from Eq. (78) is smoothly joined with Eq. (82), A and $T_{\text{Néel}}$ being considered as fitting parameters.

In the presence of both anisotropy and interlayer coupling, the situation in the critical region $x_{\bar{\sigma}}<1$ is more complicated. Consider first the case $f<\alpha$. Then at $1>x_{\bar{\sigma}}>[f/(\alpha+f)]^{1/2}$ the (sublattice) magnetization has the 3D Heisenberg behavior (80) with some coefficient $1/[1-A_0(f/\alpha)]$; at $x_{\bar{\sigma}}<[f/(\alpha+f)]^{1/2}$ the behavior $\bar{\sigma}(T)$ changes to the 3D Ising one. At $f\sim\alpha$ the 3D Heisenberg region disappears, and in the whole critical region the 3D Ising behavior takes place. With further increase of f (at $f>\alpha$), the 2D Ising critical region occurs for $1>x_{\bar{\sigma}}>x_0(f/\alpha)$, while at $x_{\bar{\sigma}}<x_0(f/\alpha)$ the 3D Ising behavior still takes place. However, the dependence $x_0(f/\alpha)$ cannot be calculated within the approaches under consideration.

Now we turn to the case of a ferromagnet. As already mentioned, in this case the dynamical part of the action cannot be generalized to arbitrary N. Thus the expressions (67)–(72) of the first order in $1/N$ (where we set $N=3$) should be considered as physically reasonable rather than strict results. The dynamical part of the action in Eq. (7) results in cutting the quasimomentum integrals at $q\sim(T/JS)^{1/2}$. The indices r can be dropped, since the quantum renormalizations are absent. Thus we have, instead of Eq. (78), for $T\gg JS\max\{f,\alpha\}$

$$\bar{\sigma}=1-\frac{T}{4\pi\rho_s^0}\left[\ln\frac{2T}{JS\Delta}+B_2\ln(1/\bar{\sigma}^2)-2+2\bar{\sigma}^2+\mathcal{O}(4\pi\rho_s^0/\bar{\sigma}^2)\right], \tag{83}$$

where $\mathcal{O}(4\pi\rho_s^0/\bar{\sigma}^2)$ terms cannot be calculated within such a consideration. For the Curie temperature we reproduce the RG result (61).

V. DISCUSSION AND COMPARISON WITH EXPERIMENTAL DATA

The above consideration provides a description of the long-range order of quantum and classical magnets in different temperature regions. Let us summarize the results obtained in the practically interesting case $N=3$. In the spin-wave and 2D-like regions, i.e., at

$$\bar{\sigma}_r\gg T/4\pi\rho_s, \quad \Gamma\gg\Delta, \tag{84}$$

TABLE I. Parameters of the equations for the (sublattice) magnetization [Eqs. (85) and (94)] for different cases, $Z_{L1}=Z_{L2}=Z_{L3}=1-T/8\pi\rho_s^0$.

	$\Gamma(T)$	$\bar{\sigma}_r$	ρ_s	f_r	α_r
Quantum AFM	T^2/c^2	$\overline{S/S_0}$	$\gamma S\overline{S_0}$	$f\overline{S_0^2}/S^2$	$\alpha\overline{S_0}/S$
Quantum FM	T/JS	$\overline{S/S}$	ρ_s^0	f	α
Classical FM, AFM	32	$\overline{S/S}$	$\rho_s^0 Z_{L1}$	fZ_{L2}^{-1}	αZ_{L3}^{-1}

we have the RG result for the relative (sublattice) magnetization,

$$\bar{\sigma}_r=1-\frac{T}{4\pi\rho_s}\left[\ln\frac{2\Gamma(T)}{\Delta(f_t,\alpha_t)}+2\ln(1/\bar{\sigma}_r)+2(1-\bar{\sigma}_r)\right], \tag{85}$$

where the function $\Delta(f,\alpha)$ is determined by Eq. (32), the temperature-renormalized values of interlayer coupling and anisotropy parameters are

$$f_t/f_r=(\alpha_t/\alpha_r)^2=\bar{\sigma}_r^2 \tag{86}$$

and the quantities $\Gamma(T),\bar{\sigma}_r,f_r,\alpha_r,\rho_s$ are given in Table I (see also Appendix A).

The corresponding equation for the magnetic ordering temperature T_M has the form

$$T_M=4\pi\rho_s\Big/\left[\ln\frac{2\Gamma(T_M)}{\Delta(f_c,\alpha_c)}+2\ln\frac{4\pi\rho_s}{T_M}+\Phi(f/\alpha)\right], \tag{87}$$

where $\Phi(x)$ is some function of order of unity (in the quantum case it is universal, i.e., does not depend on the upper cutoff parameter), f_c and α_c are the temperature-renormalized interlayer coupling and anisotropy parameters at $T=T_M$ that are determined by

$$f_c/f_r=(\alpha_c/\alpha_r)^2=(T_M/4\pi\rho_s)^2. \tag{88}$$

Since $T_M/4\pi\rho_s\sim 1/\ln(1/\Delta)\ll 1$ the temperature renormalizations are important when treating experimental data. In particular, the parameters, which are measured at different temperatures, may differ considerably.

In the case $\alpha=0$ we have

$$\bar{\sigma}_r=1-\frac{T}{4\pi\rho_s}\left[\ln\frac{\Gamma(T)}{f_r}+4\ln(1/\bar{\sigma}_r)+2(1-\bar{\sigma}_r)\right], \tag{89}$$

$$T_M=4\pi\rho_s\Big/\left[\ln\frac{\Gamma(T_M)}{f_r}+4\ln\frac{4\pi\rho_s}{T_M}+\Phi(0)\right]. \tag{90}$$

In the case $f=0$ we obtain

$$\bar{\sigma}_r=1-\frac{T}{4\pi\rho_s}\left[\ln\frac{2\Gamma(T)}{\alpha_r}+3\ln(1/\bar{\sigma}_r)+2(1-\bar{\sigma}_r)\right], \tag{91}$$

$$T_M=4\pi\rho_s\Big/\left[\ln\frac{2\Gamma(T_M)}{\alpha_r}+3\ln\frac{4\pi\rho_s}{T_M}+\Phi(\infty)\right]. \tag{92}$$

The results of solving the SSWT equations[11,12] differ from Eqs. (89)–(92) by the replacement $4(3)\to 2(1)$ for the co-

efficient at the second term in the square brackets (which yields the double-logarithmic correction to the standard SWT) in the anisotropic 2D (isotropic quasi-2D) case, respectively. Thus the role of the corrections to SSWT is more important in the isotropic quasi-2D case than in the 2D anisotropic one.

As discussed in the Introduction, the results (85) and (87) are expected to hold in the first order of the $1/M$ expansion in the CP^{M-1} model (at $M=2$).

In the temperature interval outside the critical region

$$\overline{\sigma_r^2} > T/4\pi\rho_s, \quad \Gamma \gg \Delta \tag{93}$$

the result of the $1/N$ expansion in the $O(N)$ model to the first order in $1/N$ reads

$$[1-I_2(x_{\overline{\sigma}})]\overline{\sigma}_r = 1-\frac{T}{4\pi\rho_s}\left[\ln\frac{2\Gamma(T)}{\Delta(f_r,\alpha_r)} + 2B_2\ln(1/\overline{\sigma}_r)+2(1-\overline{\sigma_r^2})+I_1(x_{\overline{\sigma}})\right], \tag{94}$$

where $x_{\overline{\sigma}}=4\pi\rho_s\overline{\sigma_r^2}/T$, B_2, and Δ are determined by Eqs. (33) and (32), and $I_{1,2}(x)$ are some functions with the asymptotics $1/x$ at large x; other quantities are given in the Table I. In particular cases $\alpha=0$ and $f=0$ the coefficient at the second term in the square brackets in Eq. (94) is two times larger than for the RG results (89) and (91). In the spin-wave and 2D-like temperature regions this is an artifact of the first-order $1/N$ expansion. At the same time, the $1/N$ expansion provides a more correct description of the crossover temperature region. Due to the difference in the crossover conditions (93) and (84), the equations for T_M have the same form [Eqs. (90) and (92)] in both approaches.

Now we discuss the experimental situation. First we consider the temperature dependence of the sublattice magnetization in La_2CuO_4 (Ref. 31), which is shown in Fig. 1. This figure presents also the results of spin-wave approximations (SWT, SSWT, and the Tyablikov theory,[30] see a more detailed discussion in Ref. 3), the RG approach, and the result of $1/N$ expansion (94). The value $\gamma \simeq 1850$ K was calculated by using the experimental data[32] while $\alpha_r = 1\times10^{-3}$ was obtained from the best fit of experimental dependence $\overline{\sigma}_r(T)$ to the spin-wave theory at low temperatures. The result of the $1/N$ expansion to first order in $1/N$ is $T_{\text{Néel}}=345$ K, which is considerably lower than for all the spin-wave approximations and is in a good agreement with the experimental value, $T_{\text{Néel}}^{\text{exp}}=325$ K. The RG approach describes correctly the dependence $\overline{\sigma}_r(T)$ in the spin-wave region ($T<300$ K) and 2D-like region (which is very narrow since α is very small) while at higher temperatures this approach overestimates $\overline{\sigma}$. At the same time, the $1/N$ expansion curve is closest to the experimental data and demonstrates a correct critical behavior. The results of the numerical solution of Eq. (94) in the temperature region (93) and the dependence (80) in the critical region turn out to be smoothly joined at the point $T=330$ K (marked by a cross).

In the crossover region ($320<T<340$ K) the theoretical $O(3)$ curve lies slightly higher than the experimental one. One may speculate that this is due to the influence of anisotropy. Fixing Δ in Eq. (94) and determining B_2 from the best fit at intermediate temperatures (see Fig. 1) one finds the values $\alpha_r=1\times10^{-4}$, $f_r=5\times10^{-4}$. This value of α is more close to the experimental data of Ref. 33. Thus our approach gives a possibilty to estimate the relative role of interlayer coupling and magnetic anisotropy in layered compounds.

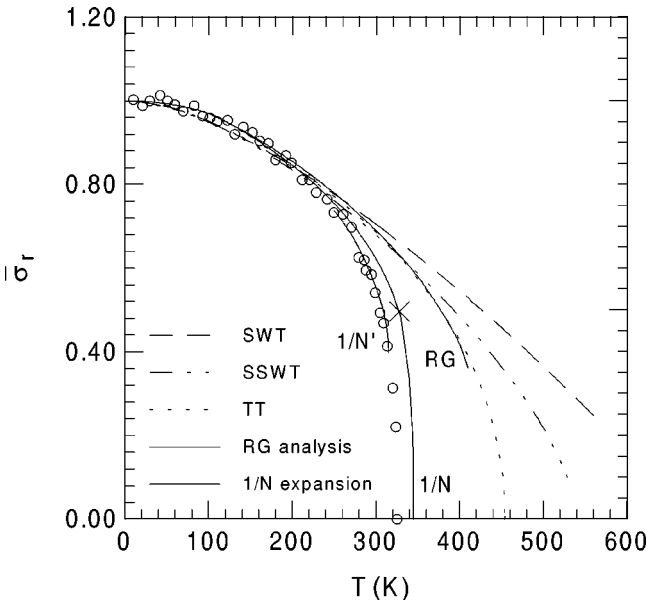

FIG. 1. The theoretical temperature dependences of the relative sublattice magnetization $\overline{\sigma_r}$ from different spin-wave approximations, RG approach [Eq. (91)], and $1/N$ expansion in the $O(N)$ model [Eqs. (78) and (80)], and the experimental points for La_2CuO_4 (Ref. 31). The RG curve is shown up to the temperature where the derivative $\partial\overline{\sigma_r}/\partial T$ diverges. The curve denoted by $1/N'$ is the best fit in the crossover temperature region to the experimental data with the anisotropy being the fitting parameter (see discussion in the text).

In the layered perovskites K_2NiF_4, Rb_2NiF_4, and K_2MnF_4 the magnetic anisotropy is known to be more important than the interlayer coupling. K_2NiF_4 has spin $S=1$, and neutron scattering data yield $|J|=102$ K and $T_{\text{Néel}}^{\text{exp}}=97.1$ K (see Ref. 1). Figure 2 shows the experimental dependence $\overline{\sigma}(T)$ (Ref. 27) and the results of the spin-wave approaches, the RG approach and the numerical solution of Eq. (94). The value $f_r=0.0088$ was obtained from the best fit of the result of SSWT to experimental data at low temperatures (this value coincides well with the experimental one $f_r=0.0084$, Ref. 1). In the spin-wave and 2D-like temperature intervals (84) ($T<80$ K) the curves corresponding to the $1/N$ expansion and RG approach lie somewhat higher than the experimental points since $T^2/f_r c^2$ in this region is not large, and the renormalized-classical description is not too good (a more accurate calculation can be performed by carrying out exact summation over the Matsubara frequencies). Bearing in mind this correction, the RG approach gives a more correct qualitative tendency than the $1/N$ expansion in the 2D-like region. At the same time, the $1/N$ expansion curve is in a good numerical agreement with experimental data. The joining procedure with the Ising critical behavior (82) may be performed in a rather wide temperature region $0.85T_{\text{Néel}}<T<0.9T_{\text{Néel}}$ and gives $A=0.01$, $T_{\text{Néel}}=91.4$ K. The width of the critical ''Ising'' region makes up about 1 K.

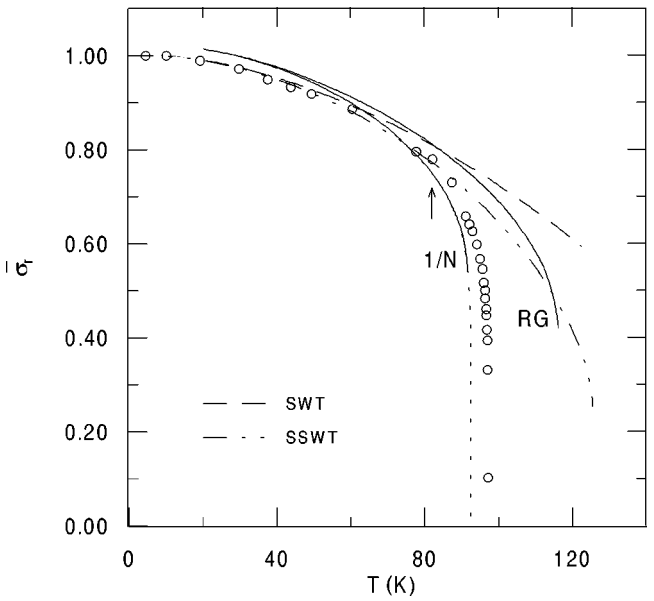

FIG. 2. The relative staggered magnetization $\overline{\sigma}_r(T)$ for K_2NiF_4 (points) as compared to the standard spin-wave theory (long-dashed line), SSWT (dot-dashed line), RG approach, and result of the solution of Eq. (78) in the intermediate-temperature region (93) (solid line). The short-dashed line shows the extrapolation of the $1/N$-expansion result to the Ising-like critical region according to Eq. (82). The boundary of the 2D-like and crossover regions is marked by an arrow.

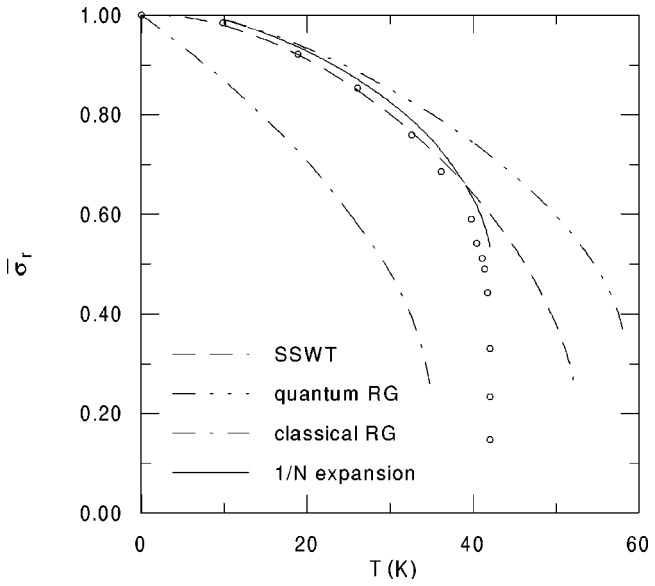

FIG. 3. The dependence $\overline{\sigma}_r(T)$ for K_2MnF_4 (points) as compared to the results of SSWT (dashed line), RG analysis in the quantum (dot-dot-dashed line), and classical (dot-dashed line) limits and solution of Eq. (78) (solid line).

Note that an account of the terms of order of $1/x_{\overline{\sigma}}$ in Eq. (78), which can be performed by analogy with the calculations of Ref. 3, gives $T_{\text{Néel}}=92.7$ K.

In the crossover region ($80<T<90$ K) the theoretical $O(3)$ curve for K_2NiF_4 lies, in contrast with the case of La_2CuO_4, slightly lower than the experimental one. This fact may be attributed to the influence of interlayer coupling. The fitting in the crossover region yields the values $\alpha_r=0.0017$, $f_r=0.0069$, which correspond to $T_{\text{Néel}}=97$ K and the bare parameters $\alpha|J|=0.1$ K, $\zeta|J|=0.76$ K. Direct experimental data for α are absent, but our estimation seems to be reasonable.

Rb_2NiF_4 has a larger magnetic anisotropy. According to Ref. 1, one has $|J|=82$ K, $|J|f_r=3.45$ K, $T_{\text{Néel}}^{\text{exp}}=94.5$ K. From the best fit of SSWT to the dependence $\overline{\sigma}_r(T)$ at low temperatures one obtains $f_r=0.046$, which is also in good agreement with the above experimental value. Then one obtains from (94) $T_{\text{Néel}}=95.5$ K.

K_2MnF_4 has spin $S=5/2$ and therefore represents a situation that is intermediate between the quantum and classical cases. Figure 3 shows a comparison of the results of different approaches with experimental data for this compound. The parameters used are $|J|=8.4$ K, $|J|f_r=0.13$ K (see Ref. 1). One can see that the $1/N$ expansion yields good results, and the experimental points lie between the quantum and classical RG curves, the quantum approximation being considerably more satisfactory. This confirms once more that it is difficult to realize the classical limit (see Appendix B). Note that SSWT, which correctly takes into account lattice effects, provides in this case better results in comparison with the RG approach. Thus an accurate treatment of such situations within continuum models requires numerical calculations of quasimomentum integrals and sums over Matsubara frequencies in Eq. (67).

Figure 4 shows a comparison of the results of SSWT and the RG approach for the magnetization of a classical magnet with the Monte Carlo calculations.[13] One can see that, except for a very narrow critical region, the RG curve is rather accurate although topological excitations are neglected. Note that the region of applicability of the RG approach in the classical case is more broad than in the quantum case, so that we need not use the large-N approach for describing the crossover to the critical region.

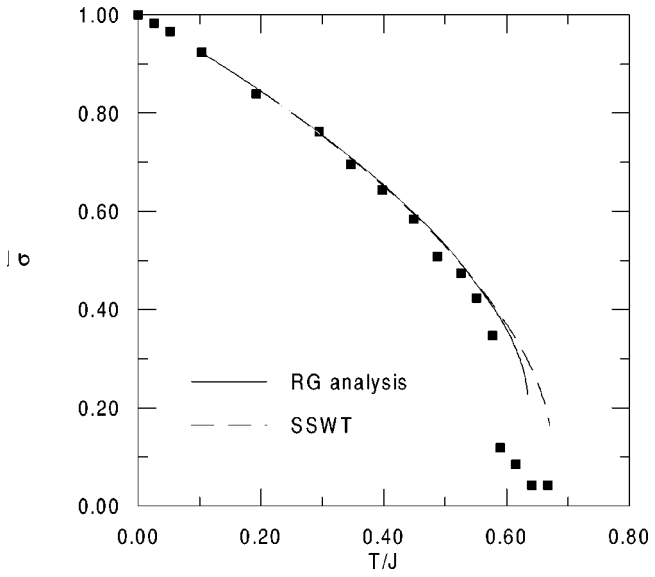

FIG. 4. The renormalization group (solid line) and SSWT (dashed line) results for the relative magnetization $\overline{\sigma}$ of a classical anisotropic 2D magnet ($\zeta=0$, $\eta=0.001$) as compared to the result of the Monte Carlo calculation.[13] The RG and SSWT curves are shown up to the temperature where $\partial\overline{\sigma}/\partial T=\infty$.

Thus the RG approach [or, equivalently, the $1/M$ expansion in the $SU(M)$ model] and the $1/N$ expansion in the $O(N)$ model turn out to give good results in different temperature regions. Whereas the first method describes well the 2D-like regime, the $1/N$ expansion describes successfully the crossover to the critical region and, in the absence of anisotropy, the critical behavior. Both methods give the same results for the ordering point up to the terms of order of $\ln(1/\Delta)$. Besides that, the $1/N$ expansion permits us to calculate nonsingular terms in the quasi-2D case.

To conclude, our results give a possibility to describe magnetic properties of real layered magnets with a rather high accuracy. The approaches applied may be useful for treating magnetic and structural phase transitions in systems with more complicated order parameters.[34]

APPENDIX A: SPIN-WAVE RESULTS FOR THE GROUND-STATE RENORMALIZATIONS IN A QUANTUM ANTIFERROMAGNET

The ground-state thermodynamic quantities of the quantum antiferromagnet can be calculated within the spin-wave theory. The result for the ground-state staggered magnetization reads[35]

$$\overline{S_0}=S-\frac{1}{2}\sum_{\mathbf{k}}\left[\frac{1}{\sqrt{1-\phi_{\mathbf{k}}^2}}-1\right]\approx S-0.1966, \tag{A1}$$

where $\phi_{\mathbf{k}}=\frac{1}{2}(\cos k_x+\cos k_y)$. The ground-state spin stiffness and spin-wave velocity to first order in $1/S$ are given by[36,8]

$$\rho_s=\gamma S\overline{S_0}, \quad c=\sqrt{8}\gamma S \tag{A2}$$

with γ being the quantum-renormalized intralayer exchange parameter determined by

$$\gamma/|J|=1+\frac{1}{2S}\sum_{\mathbf{k}}\left[1-\sqrt{1-\phi_{\mathbf{k}}^2}\right]\approx 1+\frac{0.0790}{S}. \tag{A3}$$

For the quantum-renormalized coupling constant we have $g_r=c/\rho_s$. The quantum-renormalized interlayer coupling and anisotropy parameters can be determined from the first-order $1/S$ corrections to the excitation spectrum. We have at $T=0$ and for small in-plane wave-vector components[12]

$$E_{\mathbf{k}}^2\simeq 8(\gamma S)^2\left[k_\parallel^2+\frac{2\gamma'}{\gamma}(1-\cos k_z)+\frac{\delta}{\gamma S}\right], \tag{A4}$$

where

$$\gamma'=\frac{\alpha}{2}(\overline{S_0}/S)|J| \tag{A5}$$

is the renormalized interlayer coupling and

$$\delta=(\overline{S_0}/S)^2[(2S-1)\zeta+4\eta S|J|/\gamma]|J| \tag{A6}$$

is the renormalized anisotropy. Note that in the case $\zeta,\eta\ll 1$, which is considered only, single- and two-site anisotropies lead to the same effects. Comparing the spectrum (A4) with the bare spin-wave spectrum determined from Eq. (15),

$$E_{\mathbf{k}}^2=c^2[k_\parallel^2+\alpha(1-\cos k_z)+f], \tag{A7}$$

we obtain the relation between the bare and the quantum-renormalized parameters:

$$f_r=\frac{\delta}{\gamma S}=(\overline{S_0}/S)^2\left[\frac{(2S-1)\zeta|J|}{\gamma S}+\frac{4\eta J^2}{\gamma^2}\right], \tag{A8}$$

$$\alpha_r=\frac{2\gamma'}{\gamma}=\alpha\overline{S_0}/S. \tag{A9}$$

However, it should be noted that since the spectrum (A4) contains solely renormalized parameters rather than the bare ones, $(\alpha/2)|J|$ and $[2\zeta(1-1/2S)+4\eta]|J|$, only γ' and δ can be determined experimentally.

APPENDIX B: RENORMALIZATION-GROUP ANALYSIS IN THE LATTICE $O(N)$ MODEL AND THE LIMIT OF CLASSICAL SPINS

The treatment of the partition function for the classical anisotropic quasi-2D anisotropic magnets (5) is similar to the isotropic 2D case.[18] In this case the relative temperature $t=T/(2\pi\rho_s^0)$ plays the role of a coupling constant, and we have instead of the first line of Eq. (12) the scaling relation

$$t=Z_1 t_R, \tag{B1}$$

where t_R is the renormalized temperature. The bare Green's function of the field $\boldsymbol{\pi}=\mathbf{n}-(\mathbf{nz})\mathbf{z}$ has the form

$$G^{(0)}(\mathbf{q})=\frac{1}{2\pi t}[2(2-\cos q_x a-\cos q_y a) \tag{B2}$$

$$+\alpha(1-\cos q_z a)+f+h]^{-1}, \tag{B3}$$

where a is the lattice constant. The renormalization constants can be calculated from the two-point vertex function. It is useful to represent these constants as

$$Z_i(t,a)=Z_{Li}(t)\widetilde{Z}_i(t_L,a), \tag{B4}$$

where $t_L=tZ_{L1}^{-1}$, Z_{Li} contain nonlogarithmic terms that are not changed under RG transformations, and $\widetilde{Z}_i$ contain all the other terms. We have

$$Z_{L1}=Z_{L2}=Z_{L3}=1-\pi t/2+\mathcal{O}(t^2),$$

$$Z_L=1. \tag{B5}$$

The results for $\widetilde{Z}_i$ read

$$\widetilde{Z}=1+t_L(N-1)\ln(64a\mu)+t_L^2(N-1)(N-3/2)\ln^2(64a\mu)$$

$$+\mathcal{O}(t_L^3), \tag{B6}$$

$$\widetilde{Z}_1=1+t_L(N-2)\ln(64a\mu)+t_L^2(N-2)\ln^2(64a\mu)+\mathcal{O}(t_L^3),$$

$$\widetilde{Z}_2=1-2t_L\ln(64a\mu)+\mathcal{O}(t_L^2),$$

$$\widetilde{Z}_3=1-t_L\ln(64a\mu)+\mathcal{O}(t_L^2). \tag{B7}$$

The expression for the magnetization to two-loop approximation is

$$\bar{\sigma}=1-\frac{t_L(N-1)}{4}\ln\frac{64}{\Delta(f_L,\alpha_L)}+\frac{t_L^2(3-N)(N-1)}{32}\ln^2\frac{64}{\Delta(f_L,\alpha_L)}-\frac{t_L^2(N-1)}{8}\left[1+\frac{f_L}{\sqrt{f_L^2+2\alpha_L f_L}}\right]\ln\frac{64}{\Delta(f_L,\alpha_L)},$$

where we have defined the renormalized quantities in the lattice case,

$$f_L=fZ_{L2}^{-1},\quad \alpha_L=\alpha Z_{L3}^{-1}. \tag{B8}$$

The equation for the magnetization can be derived in the same way as in Sec. II to obtain

$$\bar{\sigma}^{1/\beta_2}=1-\frac{t_L}{2}\left[(N-2)\ln\frac{64}{\Delta(f_t,\alpha_t)}+\frac{2}{\beta_2}\ln(1/\bar{\sigma})+2(1-\bar{\sigma}^{1/\beta_2})+\mathcal{O}(t_L/\bar{\sigma}^{1/\beta_2})\right]. \tag{B9}$$

Then the ordering temperature satisfies the equation

$$t_M=2\Big/\left[(N-2)\ln\frac{64}{\Delta(f_c,\alpha_c)}+2\ln(1/t_M)+\Phi_{\rm cl}(\alpha/f)\right]. \tag{B10}$$

Note that in the case $\alpha=0$ a similar expression was obtained in Ref. 23. However, the result of this work contains wrong coefficient at the second term in the square brackets of Eq. (B10) since not all two-loop corrections were taken into account.

Comparing the result for the magnetization (B9) with those of Sec. II, Eqs. (41) and (60), we can write down the criteria of applicability of the classical limit (see Sec. II) with the correct numerical factors,

$$T^2\gg 32c^2\quad (\text{AFM}),\qquad T\gg 32JS\quad (\text{FM}). \tag{B11}$$

It is difficult to satisfy these criteria in the ordered phase $T<T_M\sim 1/\ln(1/\Delta)$ at not too small Δ and $1/S$ due to the large value of the numerical factor in Eq. (B11).

*Electronic address: katanin@private.mplik.ru

[1] *Magnetic Properties of Layered Transition Metal Compounds*, edited by L. J. de Jongh (Kluwer, Dordrecht, 1989).
[2] H.-J. Elmers, Int. J. Mod. Phys. B **9**, 3118 (1995).
[3] V. Yu. Irkhin and A. A. Katanin, Phys. Rev. B **55**, 12 318 (1997).
[4] T. Oguchi and A. Honma, J. Phys. Soc. Jpn. **16**, 79 (1961).
[5] E. Rastelli, A. Tassi, and L. Reatto, J. Phys. C **7**, 1735 (1974); E. Rastelli and A. Tassi, Phys. Rev. B **11**, 4711 (1975).
[6] R. W. Wang and D. L. Mills, Phys. Rev. B **48**, 3792 (1993).
[7] M. Takahashi, Phys. Rev. **40**, 2494 (1989); Prog. Theor. Phys. Suppl. **101**, 487 (1990).
[8] A. Auerbach, *Interacting Electrons and Quantum Magnetism* (Springer-Verlag, New York, 1994).
[9] V. Yu. Irkhin, A. A. Katanin, and M. I. Katsnelson, Phys. Lett. A **157**, 295 (1991).
[10] B.-G. Liu, J. Phys.: Condens Matter **5**, 149 (1993).
[11] V. Yu. Irkhin, A. A. Katanin, and M. I. Katsnelson, Fiz. Met. Metalloved. **79**, N1, 65 (1995) [Phys. Met. Mettalogr. **79**, 42 (1995)].
[12] V. Yu. Irkhin, A. A. Katanin, and M. I. Katsnelson (unpublished).
[13] A. Levanyuk and N. Garcia, J. Phys.: Condens. Matter **4**, 10 277 (1992); P. A. Serena, N. Garcia, and A. Levanyuk, Phys. Rev. B **47**, 5027 (1993).
[14] P. A. Serena, N. Garcia, and A. Levanyuk, Phys. Rev. B **50**, 1008 (1994).
[15] A. M. Polyakov, Phys. Lett. **59B**, 79 (1975).
[16] E. Brezin and J. Zinn-Justin, Phys. Rev. B **14**, 3110 (1976).
[17] D. R. Nelson and R. A. Pelkovitz, Phys. Rev. B **16**, 2191 (1977).
[18] S. Chakravarty, B. I. Halperin, and D. R. Nelson, Phys. Rev. B **39**, 2344 (1989).
[19] A. V. Chubukov, S. Sachdev, and J. Ye, Phys. Rev. B **49**, 11 919 (1994).
[20] N. Read and S. Sachdev, Phys. Rev. B **42**, 4568 (1990).
[21] O. A. Starykh, Phys. Rev. B **50**, 16 428 (1994); A. V. Chubukov and O. A. Starykh, *ibid.* **52**, 440 (1995).
[22] V. Yu. Irkhin, A. A. Katanin, and M. I. Katsnelson, Phys. Rev. B **54**, 11 953 (1996).
[23] M. Bander and D. L. Mills, Phys. Rev. B **38**, 12 015 (1988).
[24] B.-G. Liu, Phys. Rev. B **45**, 10 771 (1992).
[25] J. R. Klauder, Phys. Rev. D **19**, 2349 (1979).
[26] F. D. M. Haldane, Phys. Lett. **93A**, 464 (1983); Phys. Rev. Lett. **50**, 1153 (1983).
[27] R. J. Birgeneau, H. J. Guggenheim, and G. Shirane, Phys. Rev. B **1**, 2211 (1970).
[28] D. Amit, *Field Theory, the Renormalization Group, and Critical Phenomena* (World Scientific, Singapore, 1984).
[29] L. D. Landau and E. M. Lifshitz, *Electrodynamics of Continuous Media* (Pergamon Press, Oxford, 1960).
[30] S. V. Tyablikov, *Methods in the Quantum Theory of Magnetism* (Plenum Press, New York, 1967).
[31] B. Keimer *et al.*, Phys. Rev. B **45**, 7430 (1992); **46**, 14 034 (1992).
[32] G. Aeppli *et al.*, Phys. Rev. Lett. **62**, 2052 (1989); K. B. Lyons *et al.*, Phys. Rev. B **37**, 2353 (1988).
[33] C. J. Peters *et al.*, Phys. Rev. B **37**, 9761 (1988); T. Thio *et al.*, *ibid.* **38**, 905 (1988); **41**, 231 (1990).
[34] R. J. Baxter, *Exactly Solved Models in Statistical Mechanics* (Academic Press, New York, 1982).
[35] P. W. Anderson, Phys. Rev. **86**, 694 (1952).
[36] T. Oguchi, Phys. Rev. **117**, 117 (1960).